INFECTION AND IMMUNITY, Jan. 2010, p. 518–526 Vol. 78, No. 1
0019-9567/10/$12.00 doi:10.1128/IAI.00257-09

Mannose Receptor-Dependent Delay in Phagosome Maturation by *Mycobacterium avium* Glycopeptidolipids▽

Lindsay Sweet,[1] Prachi P. Singh,[1] Abul K. Azad,[2] Murugesan V. S. Rajaram,[2] Larry S. Schlesinger,[2]† and Jeffrey S. Schorey[1]†*

Department of Biological Sciences, Eck Institute for Tropical Disease Research and Training, University of Notre Dame, Notre Dame, Indiana 46556,[1] and Center for Microbial Interface Biology, Division of Infectious Diseases, Department of Internal Medicine, The Ohio State University, Columbus, Ohio 43210[2]

Received 5 March 2009/Returned for modification 24 April 2009/Accepted 30 September 2009

The ability of pathogenic mycobacteria to block phagosome-lysosome fusion is critical for its pathogenesis. The molecules expressed by mycobacteria that inhibit phagosome maturation and the mechanism of this inhibition have been extensively studied. Recent work has indicated that mannosylated lipoarabinomannan (ManLAM) isolated from *Mycobacterium tuberculosis* can function to delay phagosome-lysosome fusion and that this delay requires the interaction of ManLAM with the mannose receptor (MR). However, the molecules expressed by other pathogenic mycobacteria that function to inhibit phagosome maturation have not been well described. In the present study, we show that phagosomes containing silica beads coated with glycopeptidolipids (GPLs), a major surface component of *Mycobacterium avium*, showed limited acidification and delayed recruitment of late endosomal/lysosomal markers compared to those of phosphatidylcholine-coated beads. The carbohydrate component of the GPLs was required, as beads coated only with the lipopeptide core failed to delay phagosome-lysosome fusion. Moreover, the ability of GPLs to delay phagosome maturation was dependent on the macrophage expression of the MR. Using CHO cells expressing the MR, we confirmed that the GPLs bind this receptor. Finally, human monocyte-derived macrophages knocked down for MR expression showed increased *M. avium* phagosome-lysosome fusion relative to control cells. Together, the data indicate that GPLs can function to delay phagosome-lysosome fusion and suggest that GPLs, like ManLAM, work through the MR to mediate this activity.

Mycobacterium avium, a prominent opportunistic pathogen in AIDS patients and a source of pulmonary infections in non-AIDS patients, is an intracellular pathogen which resides primarily in host macrophages. Like most pathogenic mycobacteria, *M. avium* resides within a phagosome which fails to mature to a phagolysosome (22). Phagosomes containing viable *M. avium* retain early endosomal markers such as Rab5 and the transferrin receptor but lack complete luminal acidification and recruitment of late endosomal/lysosomal markers (7, 14, 27, 28). The mechanism by which pathogenic mycobacteria are able to block phagosome-lysosome (P-L) fusion is of great interest, and how *Mycobacterium tuberculosis* performs this function has been extensively studied (27). Studies from Deretic and colleagues support that live *M. tuberculosis* blocks the normal calcium rise initiated upon a phagocytic response, the result of which leads to a diminished recruitment of type III phosphatidyl-inositol-3-kinase VPS34 to the phagosome, which limits phosphatidyl-inositol-3-phosphate (PI3P) formation and association of PI3P binding proteins such as early endosomal antigen 1 (EEA1) (8, 26). The result is a loss in the tethering and fusion of late endosomes with the mycobacterial phagosome (8, 26).

The *M. tuberculosis* surface-located mannosylated lipoarabinomannan (ManLAM) has been implicated in delaying P-L fusion. Published reports indicate that ManLAM can block the calcium influx required for stimulating phagosomal VPS34 activity (8). This ManLAM-mediated inhibition of P-L fusion appears dependent on the mannose receptor (MR), as Kang and colleagues observed that the delayed P-L fusion for ManLAM-coated microspheres was reversed when the human macrophages were preincubated with a MR-blocking antibody (12). In the same study, those authors demonstrated that the mannose caps on ManLAM were required for the MR-mediated delay in P-L fusion, as LAM with phospho-*myo*-inositol caps did not affect phagosome maturation (12). Furthermore, some species of phosphatidyl-*myo*-inositol mannosides (PIMs) expressed by *M. tuberculosis* engaged the MR, and beads coated with these PIMs also showed an MR-dependent delay in P-L fusion (25). Interestingly, expression of the MR is downregulated during gamma interferon (IFN-γ)-mediated macrophage activation (21). Thus, downregulation of the MR by IFN-γ may be one mechanism by which this cytokine promotes killing of *M. tuberculosis* by the activated macrophage.

ManLAM is also present in *M. avium*; however, its mannose cap consists of one mannose residue compared to two or three found in the ManLAM of *M. tuberculosis* (15). In addition to ManLAM, *M. avium* produces copious amounts of surface-located glycopeptidolipids (GPLs), which may mask other glycolipids (4). Because of their surface exposure, GPLs are likely candidates to interact with the host cell receptors and initiate the host response. In the present work, we found that GPLs, like ManLAM, can function to delay phagosome maturation and that this delay is MR dependent.

* Corresponding author. Mailing address: Department of Biological Sciences, University of Notre Dame, 130 Galvin Life Science Center, Notre Dame, IN 46556. Phone: (574) 631-3734. Fax: (574) 631-7413. E-mail: schorey.1@nd.edu.

† These authors contributed equally to the study.

▽ Published ahead of print on 19 October 2009.

MATERIALS AND METHODS

Lipid preparation. Total lipids were extracted from *M. avium* strain 104 in a solution of chloroform-methanol (2:1 dilution ratio) overnight at 37°C. Extracted lipids were recovered by centrifugation at 3,000 rpm for 10 min, and the lipid-containing organic layer was removed, dried down, Folch washed using endotoxin-free water to remove hydrophilic contaminants, and repeated twice, and the washed lipids were pooled. To isolate the nonserotype-specific GPLs (nsGPLs), total lipids were loaded onto a 10-cm by 20-cm Silica Gel 60 preparative thin-layer chromatography (TLC) plate (EMD Chemicals) and resolved in a developing solvent containing chloroform-methanol-water (90:10:1 dilution ratio). Side strips were cut from the developed plate and sprayed with a solution of 1% α-naphthol–5% H_2SO_4 in ethanol, which detects 6-deoxyhexoses. The most apolar band (containing native nsGPLs) and serovar 2 GPL were scraped from the TLC plate, and the silica was placed in a solution of chloroform-methanol (2:1 dilution ratio) overnight at 37°C and then centrifuged at 3,000 rpm for 10 min to remove the silica. The GPL-containing organic layer was then Folch washed, dried down, and then resuspended in chloroform-methanol (2:1 dilution ratio) at a known concentration. Initial purified samples were analyzed by gas chromatography-mass spectrometry (GC-MS) to confirm the isolation and purity of the GPLs as previously described (24). To produce the lipopeptide core (LP core), the purified nsGPLs were treated with 2 M trifluoroacetic acid (TFA) at 100°C for 2 h to hydrolyze the O-linked sugars (23). The TFA was then removed under a stream of air. The LP core was resuspended in ~5 ml of chloroform and washed with 1 ml endotoxin-free water by centrifugation at 3,000 rpm for 10 min. The water layer was removed, and both the chloroform and water layers were spotted on a TLC and visualized using the α-naphthol solution to confirm that the 6-deoxyhexoses were not present on the LP core (6-deoxyhexoses present in the water layer and not in the chloroform layer). A solution of L-α-phosphatidylcholine (PC) from the bovine brain dissolved in chloroform was purchased from Sigma, and mannosylated lipoarabinomannan (ManLAM) from *M. tuberculosis* was provided by Colorado State University.

Coating of silica beads with lipids. Silica beads (3 μm; Kisker, Germany) were washed in tissue culture (TC)-grade phosphate-buffered saline (PBS). A total of 50 μg of lipid was dissolved in approximately 100 μl of the respective favorable solvent (chloroform-methanol [2:1 dilution] for GPLs, chloroform for LP core and PC, and PBS for ManLAM). The bead suspensions were then sonicated for approximately 2 min, and organic layers were allowed to evaporate. For the dose-response experiment, 25 μg, 50 μg, or 75 μg of nsGPL or PC was used for coating the beads. ManLAM dissolved in PBS was incubated with silica beads for 2 h at 37°C, with intermittent sonication, and then ManLAM-coated beads were removed by centrifugation (3,000 rpm for 5 min). All coated beads were washed by vortexing in 1 ml PBS, and beads were removed by centrifugation, as described above (repeated twice). Beads were then incubated overnight at 4°C in 5% bovine serum albumin (BSA)-PBS to block unbound sites. Lipid-coated/BSA-blocked beads were then washed as described above, resuspended in 500 μl of 0.01% fluorescein-6-isothiocyanate (FITC) (Molecular Probes) in sterile PBS, and incubated for 2 h at 37°C. After FITC labeling, beads were washed three times, resuspended in about 200 μl of sterile PBS, and transferred to a fresh, sterile tube. To check for lipid coating, beads containing GPLs, LP core, and PC were removed from PBS and subjected to organic solvent extraction. The extract was then resolved on TLC in chloroform-methanol-water (30:8:1 dilution) and developed with aqueous 50% H_2SO_4 to visualize the lipids. To check for ManLAM-coated beads, ManLAM-coated/FITC-labeled beads were incubated with anti-ManLAM antibody (CS-35; Colorado State University) at a 1:20 dilution in 5% BSA for 4 h at room temperature, washed with PBS, and then incubated with anti-mouse Cy3-conjugated secondary antibody in 5% BSA for 2 h at room temperature. Beads were then visualized by fluorescent microscopy, and red staining was observed on ManLAM-coated/FITC-labeled beads, indicating the presence of ManLAM (not shown).

Cell culture. Bone marrow-derived macrophages (BMMΦs) were harvested from the bone marrow of 6- to 8-week-old C57BL/6 mice as described previously (14). Briefly, bone marrow was removed from the femurs, and fibroblasts and macrophages were removed by selective adhesion. Isolated monocytes were cultured for 7 days in Dulbecco's modified Eagle's medium (Gibco) supplemented with 20 mM HEPES, 10% heat-inactivated fetal calf serum (Gibco), 20% L929 cell culture supernatant, 100 U/ml penicillin, 100 μg/ml streptomycin, and 1× L-glutamine. Mature macrophages were harvested and stored in liquid nitrogen. Thawed macrophages were cultured on non-tissue culture plates for 3 to 7 days and, after one passage, were replated on TC plastic. CHO cells were thawed and plated on TC plastic in minimal essential medium alpha (MEM-α) supplemented with 10% heat-inactivated fetal calf serum, 100 U/ml penicillin, and 100 μg/ml streptomycin. CHO cells were passaged two or three times before use. Cells were seeded onto round sterile glass coverslips at 10^5 cells/coverslip and allowed to adhere for at least 24 h.

Generation of a stable CHO-K1–MR cell line. Plasmid DNA of the MR expression construct (12) was transfected into the CHO-K1 cell line (ATCC) using Lipofectamine 2000 reagent (Invitrogen), according to the manufacturer's instructions. Transfected cells were grown under selection of the antibiotic G418 (1 mg/ml), and antibiotic-resistant CHO-K1 clones were stained with anti-MR (CD206) monoclonal antibody (BD Pharmingen) and then subjected to sorting of the MR-positive cells into a single clone in a 96-well format via fluorescent activated cell sorting (FACSCalibur; BD Biosciences). The single clones were further expanded and screened for stable expression of the MR by flow cytometry and Western blotting. pcDNA3.1-based empty vector DNA was transfected to generate CHO-K1–V as the control cell line.

Phagocytosis of beads. The amount of beads/μl was determined by counting. Lipid-coated/FITC-labeled beads in sterile PBS were suspended in media (BMMΦ media or MEM-α for CHO cells). Cells were washed with PBS, and beads were added at a calculated ratio of 5 beads/cell (BMMΦ) or 50 beads/cell (CHO cells). The cells were kept on ice for 10 min, allowing beads to settle, and then transferred to the tissue culture incubator for the times indicated. For the mannan-blocking experiments, mannan from *Saccharomyces cerevisiae* (Sigma-Aldrich) was made in serum-free culture medium. The CHO-K1–MR cells were washed with PBS, and mannan was added to a final concentration of 2.5 mg/ml for 1 h prior to adding beads or the cells were left untreated. Beads coated with nsGPL were added to CHO-K1–MR cells, and 1 h later, cells were washed extensively with PBS and fixed with 2% paraformaldehyde. For the trypan blue experiments, BMMΦs were seeded on glass coverslips at 5×10^4/well and allowed to adhere for 24 h. nsGPL- or PC-coated beads were added to BMMΦs, allowed to settle on ice, and then transferred to the tissue culture incubator for the times indicated. The cells were washed with PBS, and trypan blue was added to cells (1.5-mg/ml final concentration) for 4 min. The cells were again washed four times with PBS and fixed with 2% paraformaldehyde, and the FITC-labeled beads were visualized by fluorescent microscopy. The number of phagocytosed beads was quantified with a minimum of 100 beads, counted using at least three fields per sample.

LysoTracker staining. LysoTracker red (Molecular Probes) was directly added to media at a 1:10,000 dilution and incubated with BMMΦs or CHO cells for up to 24 h prior to addition of beads, as well as during bead phagocytosis. Cells were then washed in PBS and fixed at various time points in 2% paraformaldehyde (Sigma) in PBS.

Immunofluorescence labeling. Cells with phagocytosed beads were fixed at various time points as described above. Fixed cells were permeabilized with 0.02% Triton X-100 (Sigma), blocked with 2% BSA and 2% gelatin (Sigma), and washed with 1% BSA in PBS. The anti-mouse monoclonal antibodies against lysosome-associated membrane protein-1 (LAMP-1) and LAMP-2 (1D4B and ABL-93, respectively; Developmental Hybridoma Bank) were used at a 1:200 dilution, and the anti-mouse monoclonal antibody against transferrin receptor (sc-9099; Santa Cruz) was used at a 1:50 dilution. All primary antibodies were incubated in 0.15% gelatin and 23% horse serum in PBS for 2 h at room temperature. Secondary antibodies conjugated with Cy3 were used at a dilution of 1:600 in 0.15% gelatin and 23% horse serum in PBS for 1 h at room temperature. Coverslips were mounted in mounting media containing glycerin and *n*-propyl gallate and then visualized using a Zeiss Observer microscope system with Apotome. Fluorescent images were taken sequentially in the FITC and Cy3 channels, the images were merged in PowerPoint, and the number of beads colocalizing with LysoTracker red, LAMP-1, or LAMP-2 was determined. A minimum of 100 beads were counted per experiment in a minimum of three fields for each slide.

Isolation of human macrophages and knockdown of the MR. Peripheral blood mononuclear cells (PBMCs) were isolated from blood from healthy donors (using an approved protocol by The Ohio State University Institutional Review Board) and cultivated for 5 days to obtain monocyte-derived macrophages (MDMs) as described previously (11). Knockdown of the MR in MDMs was performed using the Nucleofector II device and the human macrophage Nucleofector kit (Lonza, Germany) (M. V. S. Rajaram, J. Morris, M. Brooks, J. B. Torrelles, A. K. Azad, and L. S. Schlesinger, submitted for publication) with a pool of three MR-specific small interfering RNA (siRNA) oligos (MR1, AAG TGGTACGCAGATTGCACG; MR2, GCAGTCCTTTCCGATATTTGA; and MR3, AAGGGCAACACCACTTTAAAT). Scramble siRNA (Dharmacon) was used as a negative control for MR knockdown.

Western blotting. MDMs were lysed in TN1 lysis buffer (140 mM NaCl; 50 mM Tris-HCl, pH 8.0; 10 mM EDTA; 10 mM $Na_4P_2O_7$; 10 mM NaF; 1% Triton X-100; 125 mM NaCl; 10 mM Na_3VO_4; and protease inhibitor cocktail) for 10 min on ice. Cell lysates were centrifuged at 4°C, and the supernatant was used as

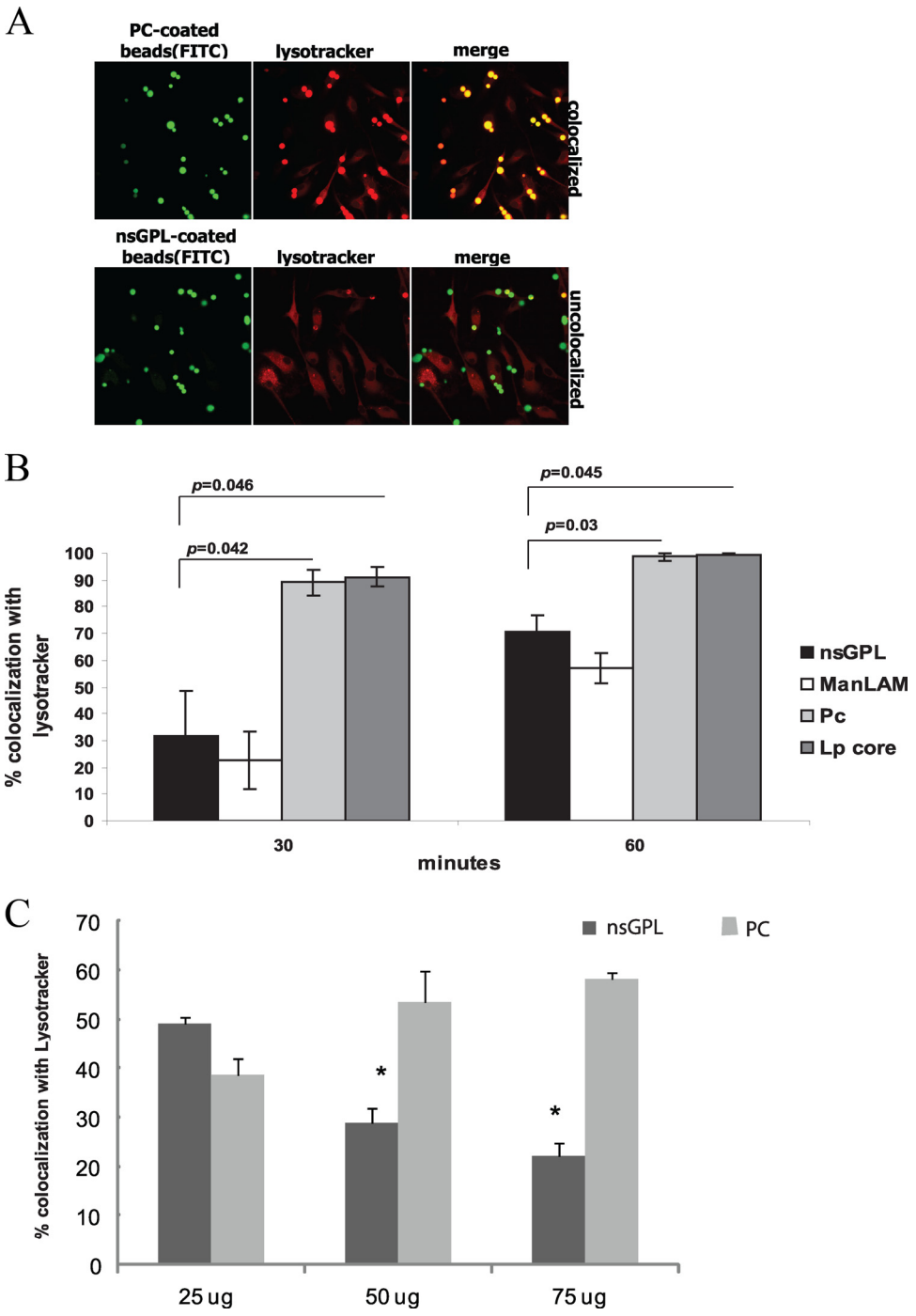

FIG. 1. GPL-coated beads show delayed colocalization with LysoTracker red. (A) Confocal images depicting macrophages stained with LysoTracker red containing nonspecific GPLs or PC-coated beads at 30 min postphagocytosis. In merged images, colocalized beads appear yellow, and noncolocalized beads remain green. (B) Percent colocalization of lipid-coated beads at 30 and 60 min postphagocytosis. Three separate experiments were conducted, error bars represent SEM, and asterisks indicate statistical significance at $P \leq 0.05$ compared to PC-coated beads. (C) Percent colocalization of lipid-coated beads with LysoTracker red at 30 min postphagocytosis using beads coated with the indicted concentrations of nsGPL or PC. Two separate experiments were conducted, with P values < 0.001. Beads were coated with nsGPLs from *M. avium* 104, ManLAM from *M. tuberculosis*, PC, and the GPL lipopeptide core (LP core).

the source of soluble proteins. Total soluble proteins were separated by 10% sodium dodecyl sulfate-polyacrylamide gel electrophoresis (SDS-PAGE) and then transferred to nitrocellulose. The blot was incubated with anti-human MR rabbit polyclonal antibody and then with horseradish peroxidase (HRP)-conjugated IgG secondary antibody (both from Santa Cruz). The same blot was reprobed with a β-actin antibody (Santa Cruz) as the loading control. The blots were developed on X-ray film by using an enhanced chemiluminescence device.

Human macrophage cell association and P-L fusion assays. Following siRNA nucleofection, MDMs were plated onto glass coverslips in a 24-well tissue culture plate (~2×10^5 cells/well) and incubated for 36 h, and subsequently FITC-

labeled *M. avium* was added to the MDM monolayers (multiplicity of infection [MOI] optimized to enable 10 to 20 bacteria/cell). To allow for synchronized phagocytosis, monolayers were placed at 4°C for 10 min and centrifuged briefly, followed by incubation at 37°C for 2 h. Following washing and fixation with 2% paraformaldehyde, MDMs were permeabilized with 100% methanol (11). The MDM monolayers on coverslips were incubated with anti-human MR monoclonal (BD Pharmingen) and CD63 rabbit polyclonal (Santa Cruz) antibodies, followed by staining with Alexa Fluor 647- and 546-conjugated secondary antibodies, respectively. The samples were processed for confocal microscopy to enumerate cell-associated bacteria and the colocalization of bacteria with the lysosomal marker CD63 (P-L fusion) as described previously (12). Each sample from two independent blood donors was processed on duplicate or triplicate coverslips.

Statistical analyses. Data were analyzed by one-tailed or paired Student's *t* test. Statistical significance was assumed at *P* values of ≤0.05. For all immunofluorescence, three separate experiments were conducted, and error bars represent standard errors of the means (SEM).

RESULTS

GPLs can function to delay phagosome maturation. *M. avium* expresses serotype-specific GPLs and apolar or nonserotype-specific GPLs (nsGPLs). The nsGPLs make up the core of the GPL and consist of a fatty acyl chain that is *N*-linked to a tripeptide-amino-alcohol core containing D-phenyl-alanine, D-*allo*-threonine, D-alanine, and L-alaninol. The *allo*-threonine is glycosidically linked to a 6-deoxy-α-L-talose (6-deoxytalose), and the alaninol is glycosidically linked to a methylated α-L-rhamnose (rhamnose). Serotype-specific GPLs are produced by the addition of sugars glycosidically linked to the 6-deoxytalose of the nsGPL, and the composition of these additional carbohydrates determines the *M. avium* serotype. Nevertheless, all *M. avium* strains express surface-exposed nsGPLs, and in most cases, this constitutes the bulk of the expressed GPLs. Therefore, we used the nsGPLs for the majority of our studies. In the initial experiments, nsGPLs isolated from *M. avium* 104 or *M. tuberculosis* ManLAM were coated onto silica beads, as described in Materials and Methods. Beads were also coated with L-α-phosphatidylcholine (PC), as a negative control, or with the lipopeptide core (LP core) of the GPL. The beads were then prelabeled with FITC and added to bone marrow-derived macrophages (BMMΦs). Colocalization between LysoTracker red and FITC-labeled beads was visualized by fluorescence microscopy (Fig. 1A). The number of beads colocalized with LysoTracker red was quantified at each time point. Phagosomes containing beads coated with nsGPLs showed more limited acidification, as defined by positive staining with LysoTracker red, compared to that of phagosomes containing PC- or LP core-coated beads (Fig. 1B). As observed previously, phagosomes containing ManLAM-coated beads also showed delayed acidification (7) (Fig. 1B). The differences were most pronounced at 30 min postphagocytosis. The ability of nsGPL to limit LysoTracker red staining of bead-containing phagosomes was dose dependent (Fig. 1C). We also tested serotype 2 GPL in this assay and observed similar results (data not shown), suggesting that nsGPLs have the structural information required to delay phagosome acidification and that the presence of additional sugars on the 6-deoxytalose does not interfere with this process.

To further confirm the delay in phagosome maturation for beads coated with nsGPL, we compared the differently coated beads for their recruitment of lysosome-associated membrane protein-1 (LAMP-1) and LAMP-2. Colocalization of beads

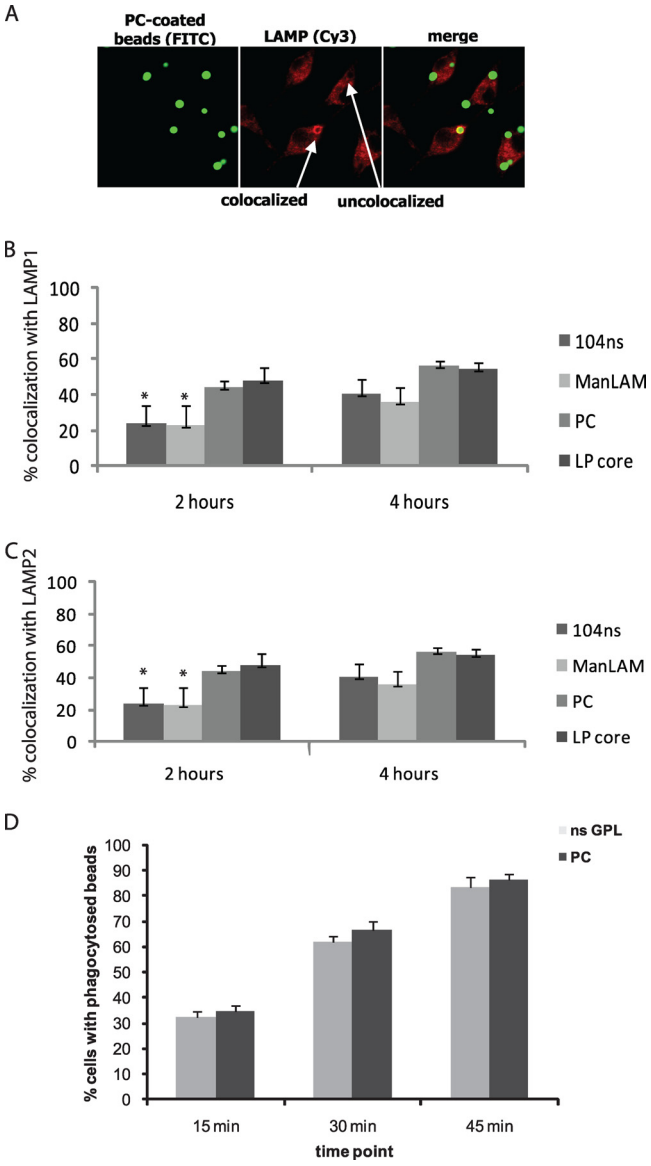

FIG. 2. Delayed colocalization of GPL-coated beads with LAMP. (A) PC-coated beads at 2 h postphagocytosis. Colocalization with LAMP proteins appears as a distinct ring surrounding the bead. (B, C) Colocalization of beads with LAMP-1 (B) and LAMP-2 (C) at 2 and 4 h postphagocytosis. Three separate experiments were conducted, error bars represent SEM, and asterisks indicate statistical significance at $P \leq 0.05$ compared to PC-coated beads. (D) Number of BMMΦs containing phagocytosed nsGPL-coated or PC-coated beads at 15, 30, and 45 min post-bead treatment. Beads were coated with nsGPLs from *M. avium* 104, ManLAM from *M. tuberculosis*, PC, and the GPL lipopeptide core (LP core).

with LAMP proteins was determined by identifying beads surrounded by a distinct "ring" (Fig. 2A). Both nsGPL- and ManLAM-coated beads showed diminished colocalization with LAMP-1 (Fig. 2B) and LAMP-2 (Fig. 2C) compared to that of PC-coated and LP core-coated beads at 2 h postphagocytosis. However, at 4 h postphagocytosis, there was no significant difference between the nsGPL-coated and control beads, with respect to both LAMP proteins (Fig. 2B and C). The observed differences in colocalization were not due to variations in the

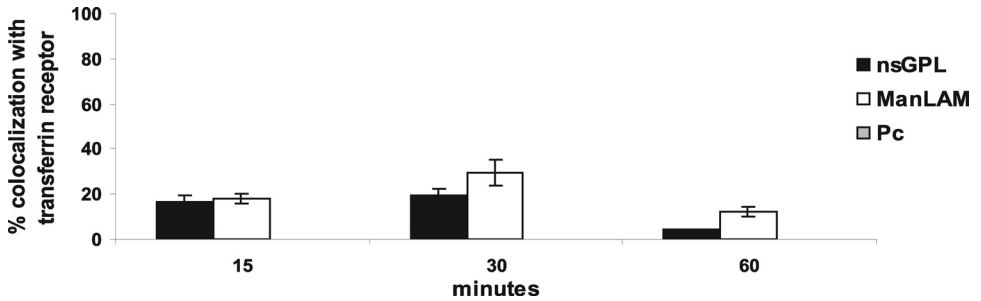

FIG. 3. Prolonged colocalization of GPL-coated beads with the transferrin receptor (TR). Beads coated with nsGPLs from *M. avium* 104, ManLAM from *M. tuberculosis*, and PC were phagocytosed by macrophages for the indicated times and analyzed for TR colocalization by fluorescent microscopy. Three separate experiments were conducted, and error bars represent SEM.

rate of phagocytosis, as the numbers of phagocytosed PC- and nsGPL-coated beads were similar at all time points tested (Fig. 2D).

The data with LysoTracker red, LAMP-1, and LAMP-2 suggested that phagosomes containing beads coated with nsGPLs or ManLAM were delayed in their maturation. Therefore, we predict that these phagosomes will show prolonged colocalization with early endosomal markers such as the transferrin receptor (TR). The TR is known to transiently colocalize with early phagosomes during its recycling back to the plasma membrane (5, 22). Moreover, previous studies have shown the TR to be retained on *M. avium* and *M. tuberculosis* phagosomes (5, 14). At 15 min postphagocytosis, a small percentage of phagosomes containing nsGPL-coated beads and ManLAM-coated beads were positive for the TR (Fig. 3). After 30 min, this number increased to ~20% for nsGPL-coated beads and to ~30% for ManLAM-coated beads but subsequently decreased by 1 hour postphagocytosis (Fig. 3). Notably, we did not observe colocalization between the phagosomes containing the PC-coated beads and the TR at any of these time points (Fig. 3). Since nearly 90% of PC-coated-bead phagosomes were acidified as early as 30 min postphagocytosis (Fig. 1B), it is likely that trafficking of the PC-coated beads occurred too quickly to observe TR colocalization by immunofluorescence. Although the phagosomes containing nsGPL- or ManLAM-coated beads also matured, the data suggest that the maturation was sufficiently delayed to observe TR colocalization.

The delay in phagosome maturation by nsGPL is dependent on the mannose receptor. As previous studies implicated a role for the mannose receptor in ManLAM-mediated delay in phagosome maturation (8, 12), we tested whether this also applied to the nsGPL-mediated delay. As shown in Fig. 4A, the observed difference in LysoTracker red staining at 30 min between phagosomes containing nsGPL- and those containing PC- or LP core-coated beads was lost when MR-deficient BMMΦs were used. By 60 min postphagocytosis, no significant difference between wild-type (WT) and MR-deficient BMMΦs was observed (Fig. 4B). As anticipated, ManLAM-mediated delay in phagosome acidification was also dependent on the MR (Fig. 4A). The requirement of the MR in nsGPL-mediated delay in phagosome maturation was further confirmed, as LAMP-1 colocalization at 2 hours postphagocytosis with nsGPL-coated beads was markedly increased when using BMMΦs isolated from MR-deficient mice rather than WT mice (Fig. 4C). However, at 4 h, the percent colocalization had reached comparable levels (Fig. 4D). Similar results were seen with LAMP-2 (data not shown).

nsGPL- and ManLAM-coated beads associate with CHO cells expressing the human MR. The above-described experiments suggest that nsGPLs can interact with the MR; however, this has not been directly evaluated. Therefore, wild-type CHO cells (CHO-K1–V) and CHO cells expressing the human MR (CHO-K1–MR) were used to determine whether nsGPLs could physically interact with the MR. nsGPL-, ManLAM- and PC-coated beads were added to both CHO-K1–V and CHO-K1–MR cells (preincubated with LysoTracker red to visualize the cells), and the number of cells with bound or ingested beads was visualized by fluorescent microscopy. Approximately 20% of the CHO-K1–V cells were positive for lipid-coated beads, regardless of the type of lipid. This significantly increased when the CHO-K1–MR cells were exposed to nsGPL-coated beads (Fig. 5A). However, there was no significant difference in the amount of PC-coated beads bound to or ingested by the different CHO cell lines. Moreover, the binding of the nsGPL-coated beads to CHO-K1–MR cells was significantly diminished in the presence of mannan, suggesting that GPLs interact with the sugar binding domain on the MR (Fig. 5B). These results show that nsGPL-coated beads bound more readily to cells expressing the human MR, suggesting that nsGPLs are a ligand for the MR. As expected ManLAM-coated beads also bound readily to CHO-K1–MR cells, as ManLAM is a known ligand for the MR (11, 12).

***M. avium* shows delayed phagosome-lysosome fusion in human monocyte-derived macrophages rendered diminished in MR expression.** Since our results indicate that GPLs can bind to the MR and that this binding is required for the delayed phagosome maturation observed for GPL-coated beads, we wanted to evaluate whether *M. avium*'s engagement of the MR also functions to limit its phagosome-lysosome fusion. In our initial experiments, we used WT and MR-deficient murine bone marrow-derived macrophages. We infected these cells with *M. avium* and looked for differences over time in bacteria transport to a LysoTracker red-positive compartment, as a measure of a late endosome or lysosomal compartment. We did not observe any difference in the staining of *M. avium* for LysoTracker red between WT and MR-deficient macrophages (data not shown).

Previous studies addressing the role of the MR in *M. tuberculosis* trafficking was performed in human monocyte-derived macrophages (MDMs) whose MR was blocked either by

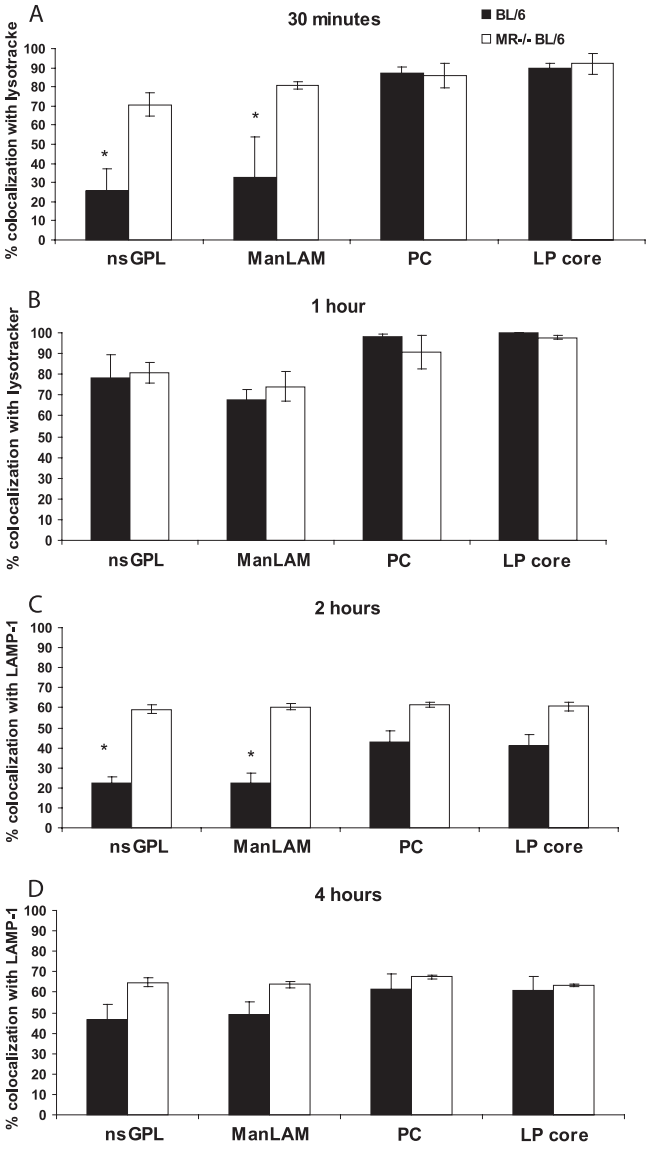

FIG. 4. Delay in acidification and recruitment of LAMP-1 to bead phagosomes is mannose receptor (MR) dependent. Colocalization of beads with LysoTracker red at 30 min (A) and 60 min (B) postphagocytosis. Colocalization of beads with LAMP-1 at 2 h (C) and 4 h (D) postphagocytosis. Percent colocalization determined in macrophages from wild-type mice (BL/6) and MR knockout C57BL/6 mice ($MR^{-/-}$ BL/6). Three separate experiments were conducted, error bars represent SEM, and asterisks indicate statistical significance at $P \leq 0.05$ when comparing values obtained from BL/6 macrophages and those obtained from $MR^{-/-}$ BL/6 macrophages for corresponding lipid-coated beads. Beads were coated with nsGPLs from *M. avium* 104, ManLAM from *M. tuberculosis*, PC, and the GPL lipopeptide core (Lp core).

anti-MR antibody or by mannan. In these studies, *M. tuberculosis* was found to show increased phagosome-lysosome fusion in cells whose MR was blocked (12). To determine if *M. avium* transport in human MDMs was also affected by interaction with the MR, we used siRNA to knockdown MR expression in MDMs, a new and previously unpublished approach to limit MR expression in human primary cells (Fig. 6A). Interestingly, we found a significant increase in the number of lysosomal marker CD63-positive *M. avium* phagosomes in MR-knockdown MDMs relative to control scrambled siRNA-treated cells (Fig. 6B and C).

DISCUSSION

GPLs have been shown to modulate cellular responses. Studies by Horgen et al. showed that pretreatment of human peripheral blood mononuclear cells (PBMCs) with serovar 4 and 8 GPLs inhibited the response of these cells to phorbol myristate acetate (PMA), a potent inducer of T-cell activation (10). Additional studies have addressed whether GPLs can induce or modulate a proinflammatory response. Total lipid and serovar-specific GPL (ssGPL) fractions have been observed to induce the release of various proinflammatory mediators, such as prostaglandins, leukotrienes, interleukin-1 (IL-1), IL-6, and tumor necrosis factor alpha (TNF-α) (1, 2, 10, 18, 23). This proinflammatory response appears to be structure specific, as only certain ssGPLs were active (1, 23). This suggests that slight structural modifications can alter the way in which the GPL interacts with host cell receptors. In vivo studies have also implicated a role for GPLs in *M. avium* pathogenesis. Studies by Krzywinska et al. showed that an *mtfD*-deficient *M. avium* 104 strain, which has an unusual GPL profile and produces undermethylated GPLs, was attenuated in a mouse model of infection (16). These observations suggest that modifying GPL structure can significantly change its biological activity, even in the context of whole mycobacteria.

Therefore, we and others have begun to dissect the interactions between GPLs and macrophages, as well as other host cells (18, 20, 23). We have observed that the proinflammatory response induced by GPLs is MyD88- and Toll-like receptor 2 (TLR2) dependent, suggesting that certain GPLs have the necessary structure to signal through this receptor (23). These results corroborate other studies which have shown that *M. avium* can stimulate a proinflammatory response in macrophages through TLR2 and that TLR2-deficient mice are more susceptible to an *M. avium* infection than wild-type mice (6). We have also found that a rough *M. avium* 2151 morphological variant, which lacks GPL expression and is avirulent in mice (3), does not inhibit phagosome-lysosome fusion and is readily killed by nonactivated BMMΦs. However, it is unclear from these studies whether the effects were due directly to the loss of GPLs or due to global changes in the cell wall associated with the loss of GPL.

Kano et al. have demonstrated that heat-killed *Staphylococcus aureus* coated with serovar 4 GPL shows increased phagocytosis by PBMCs compared to that of serovar 9 GPL-coated or uncoated bacteria (13). Serovar 4 GPL-coated *S. aureus* ingested by THP-1 cells also showed a delayed phagosome maturation, defined by LysoTracker red staining, compared to that of uncoated or lipopeptide-coated *S. aureus* (13). These data suggest that GPLs may function in limiting phagosome maturation; however, it was unclear from these studies how components of the *S. aureus* cell wall may be modulating this process, as this bacterium has been shown to stimulate the innate immune response via other receptors (9, 17). Moreover, the experiments were performed using deacetylated GPLs and therefore do not provide information about the function of the native molecules (13). In the present study we used nsGPLs, as

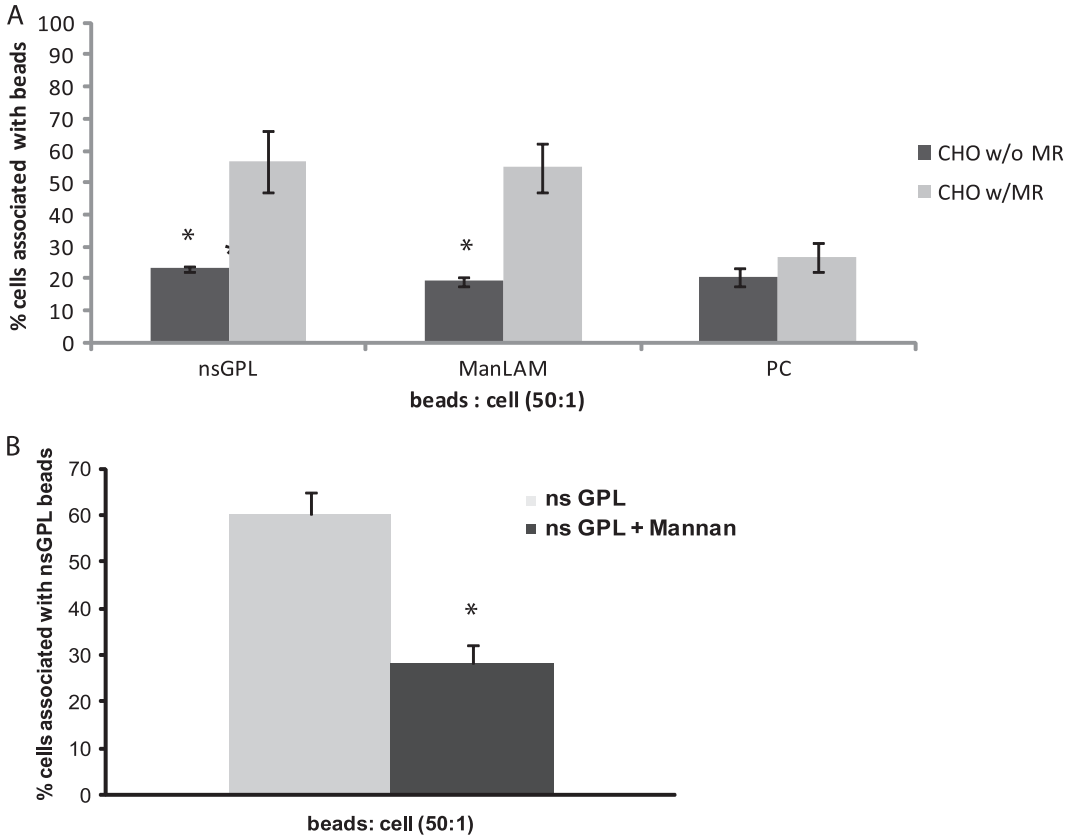

FIG. 5. nsGPLs bind CHO cells expressing the mannose receptor (MR), and the binding is blocked by mannan. CHO cells transfected with the human mannose receptor (CHO-K1–MR) or mock-transfected CHO cells (CHO-K1–V) were incubated with lipid-coated beads for 1 h at a ratio of 50 beads/cell. (A) Quantification by fluorescence microscopy of the number of CHO cells containing attached/phagocytosed FITC-labeled beads coated with nsGPL, ManLAM, or PC. Three separate experiments were conducted, error bars represent SEM, and asterisks indicate statistical significance at $P \leq 0.05$ when comparing CHO-K1–MR and CHO-K1–V for corresponding lipid-coated beads. (B) CHO-K1–MR cells incubated in the presence or absence of 2.5 mg/ml mannan were exposed to nsGPL-coated beads for 1 h at a ratio of 50 beads/cell. The number of beads attached/phagocytosed by the CHO cells was quantified by fluorescence microscopy. Three separate experiments were conducted, error bars represent SEM, and asterisks indicate statistical significance at $P < 0.0001$.

they are expressed by all *M. avium* serotypes, and we also isolated nsGPLs in their native conformations. Like GPL-coated *S. aureus*, we observed delayed LysoTracker red staining of phagosomes containing the nsGPL-coated beads compared to that of beads coated with PC or the lipopeptide core. We extended these results, showing retention of the early endosomal marker TR on phagosomes containing nsGPL-coated beads, and delayed colocalization with the late endosomal markers LAMP-1 and LAMP-2.

Since the MR has been implicated in the ability of ManLAM to affect phagosome maturation, we tested its role in the nsGPL-mediated delay in phagosome maturation. Like what was observed for ManLAM, the maturation block by nsGPL was dependent on the mannose receptor. These results imply that GPLs can bind the MR, and our results using the MR-expressing CHO cells directly support this prediction. How do GPLs interact with the MR since GPLs do not contain a mannose cap? The nsGPLs contain 6-deoxy-α-L-talose (6-deoxytalose) and 6-deoxy-α-L-mannose (rhamnose). It appears that the presence of these sugars is important for the nsGPLs' ability to delay acidification and recruitment of lysosomal markers in wild-type macrophages, as the lipopeptide core failed to affect phagosome maturation. However, the determination of which sugars and structural modifications (i.e., glycosylation, acetylation, etc.) are required for binding to the MR awaits further study.

An important question is whether GPLs function to delay phagosome maturation in the context of intact *M. avium*. Unfortunately, mutants of *M. avium* which lack GPLs have altered cells walls and therefore cannot be used to address GPLs' role in modulating the phagosome maturation process. Since nsGPLs can bind the MR and this receptor functions to limit phagosome maturation of GPL-coated beads, we sought to evaluate whether phagosome maturation for GPL-expressing *M. avium* differed in the presence or absence of the macrophage MR. Interestingly, although we did not observe any difference between WT and MR-deficient murine macrophages, we did observe increased phagosome-lysosome fusion when we used human MDMs whose MR expression was knocked down by siRNA. Why the difference between murine and human macrophages? It could relate to differences between species in signaling response downstream of MR engagement. Unfortunately, little is known about how signals are transmitted through the MR, since it lacks any known motifs

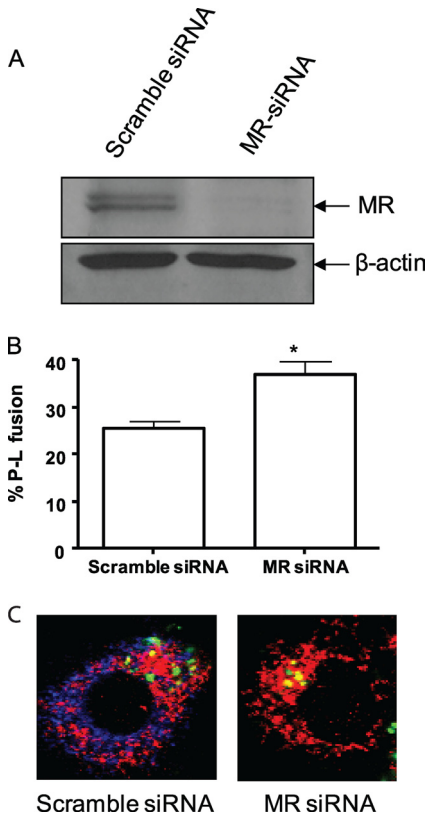

FIG. 6. MR knockdown leads to increased phagosome-lysosome fusion for *M. avium* in human MDMs. (A) Western blot of lysates from scramble (control) siRNA- and MR siRNA-treated macrophages. Shown is a representative blot (Western blots performed with each macrophage experiment to confirm MR knockdown). Following scramble (control) or MR siRNA nucleofection for 36 h, FITC-labeled *M. avium* was added to MDM monolayers on glass coverslips and allowed to undergo synchronized phagocytosis for 2 h. Cell monolayers were fixed, permeabilized, and stained with anti-human MR and CD63 antibodies, followed by staining with Alexa Fluor 647- and 546-conjugated secondary antibodies, respectively. (B) Percent phagosome-lysosome (P-L) fusion assessed based on the colocalization of bacteria with the lysosomal marker CD63. Shown are the means ± SEM from two independent experiments, each performed in duplicate or triplicate. *, $P < 0.05$ using the paired, one-tailed Student *t* test. (C) Representative confocal images of MDMs treated with siRNA and infected with *M. avium* (green, *M. avium*; red, CD63; blue, MR).

on its cytoplasmic tail and therefore is presumed to interact with yet unknown transmembrane proteins for signaling. Another possibility is differences in receptor expression between human and mouse macrophages. For example, most unstimulated human macrophages (including the MDMs used in the current work) do not express DC-SIGN, while mouse macrophages express various SIGNRs. SIGNR3 is thought to be the ortholog that is most similar to DC-SIGN (19). Since SIGNR3 and other SIGNRs can bind the same sugars as the MR, it is possible that the loss of the MR in mouse macrophages is compensated by expression of one or more of the SIGNRs, a mechanism that cannot occur in human macrophages. Nevertheless, our results are analogous to those observed for *M. tuberculosis* and suggest a general role for the MR upon engagement by pathogenic mycobacteria in subverting the phagosome maturation process in human macrophages. Moreover, since GPLs are (i) found in high abundance on the *M. avium* cell wall, (ii) known to be exposed to the extracellular environment, and (iii) a ligand for the MR, we hypothesize that GPLs, through their engagement of the MR, function to delay phagosome maturation. However, further studies using *M. avium* strains that express GPLs which bind or fail to bind MR are needed to test this hypothesis. Nevertheless, blocking phagosome maturation is clearly multifactorial and likely involves other mycobacterial components and other host receptors as well as possibly other MR ligands.

The mechanism by which the nsGPLs, ManLAM, or other mycobacterial components may function to delay phagosome maturation is unclear. Previous studies for ManLAM suggest that this glycolipid can inhibit the calcium flux normally induced upon phagocytosis (8). This increased calcium is required for the activation of calmodulin kinase II, which in turn promotes VPS34-mediated production of PI3P. Production of PI3P is required for recruitment of EEA1 and other PI3P binding proteins that promote delivery of lysosomal components from the *trans*-Golgi network to the maturing phagosome (8). However, in our studies we did not observe any kinetic differences in EEA1 recruitment to phagosomes containing nsGPL-coated beads compared to those containing PC-coated beads (data not shown). Our study and others (11, 12) have also implicated the mannose receptor (MR) in regulating phagosome maturation. However, whether engagement of the MR alters calcium production or calmodulin kinase II activation following mycobacterial infection has not been addressed (12).

In summary, our results indicate that nsGPLs can function to delay phagosome maturation. Our data also support a role for the MR in this process; however, more information about how GPLs may physically interact with the MR is needed. In addition, we have also shown that certain nsGPL structural variants can signal through Toll-like receptor 2 (TLR2) (24), but how GPL-mediated signaling through TLR2 affects phagosome maturation has not been addressed. Questions also remain as to how engagement of the MR during the phagocytic process results in delayed phagosome maturation. Finally, further work is needed to determine whether engagement of the mannose receptor by intramacrophage pathogens is a common mechanism to modulate phagosome maturation.

ACKNOWLEDGMENTS

This work was supported through grants AI056979 and AI052439 (to J.S.S.) and grant AI052458 (to L.S.S.) from the National Institute of Allergy and Infectious Diseases.

ManLAM was generously provided from Colorado State University as part of NIH/NIAID contract HHSN266200400091C, titled "Tuberculosis Vaccine Testing and Research Materials."

The 1D4B and ABL-93 monoclonal antibodies developed by J. T. August were obtained from the Developmental Studies Hybridoma Bank developed under the auspices of the NICLD and maintained at the University of Iowa, Department of Biology, Iowa City, IA 52242.

REFERENCES

1. **Barrow, W. W., T. L. Davis, E. L. Wright, V. Labrousse, M. Bachelet, and N. Rastogi.** 1995. Immunomodulatory spectrum of lipids associated with Mycobacterium avium serovar 8. Infect. Immun. **63:**126–133.
2. **Barrow, W. W., J. P. de Sousa, T. L. Davis, E. L. Wright, M. Bachelet, and N. Rastogi.** 1993. Immunomodulation of human peripheral blood mononuclear cell functions by defined lipid fractions of Mycobacterium avium. Infect. Immun. **61:**5286–5293.

3. **Bhatnagar, S., and J. S. Schorey.** 2006. Elevated mitogen-activated protein kinase signalling and increased macrophage activation in cells infected with a glycopeptidolipid-deficient Mycobacterium avium. Cell. Microbiol. **8:**85–96.
4. **Chatterjee, D., and K. H. Khoo.** 2001. The surface glycopeptidolipids of mycobacteria: structures and biological properties. Cell. Mol. Life Sci. **58:** 2018–2042.
5. **Clemens, D. L., and M. A. Horwitz.** 1996. The Mycobacterium tuberculosis phagosome interacts with early endosomes and is accessible to exogenously administered transferrin. J. Exp. Med. **184:**1349–1355.
6. **Feng, C. G., C. A. Scanga, C. M. Collazo-Custodio, A. W. Cheever, S. Hieny, P. Caspar, and A. Sher.** 2003. Mice lacking myeloid differentiation factor 88 display profound defects in host resistance and immune responses to Mycobacterium avium infection not exhibited by Toll-like receptor 2 (TLR2)- and TLR4-deficient animals. J. Immunol. **171:**4758–4764.
7. **Fratti, R. A., J. M. Backer, J. Gruenberg, S. Corvera, and V. Deretic.** 2001. Role of phosphatidylinositol 3-kinase and Rab5 effectors in phagosomal biogenesis and mycobacterial phagosome maturation arrest. J. Cell Biol. **154:**631–644.
8. **Fratti, R. A., J. Chua, I. Vergne, and V. Deretic.** 2003. Mycobacterium tuberculosis glycosylated phosphatidylinositol causes phagosome maturation arrest. Proc. Natl. Acad. Sci. U. S. A. **100:**5437–5442.
9. **Hashimoto, M., K. Tawaratsumida, H. Kariya, K. Aoyama, T. Tamura, and Y. Suda.** 2006. Lipoprotein is a predominant Toll-like receptor 2 ligand in Staphylococcus aureus cell wall components. Int. Immunol. **18:**355–362.
10. **Horgen, L., E. L. Barrow, W. W. Barrow, and N. Rastogi.** 2000. Exposure of human peripheral blood mononuclear cells to total lipids and serovar-specific glycopeptidolipids from Mycobacterium avium serovars 4 and 8 results in inhibition of TH1-type responses. Microb. Pathog. **29:**9–16.
11. **Kang, B. K., and L. S. Schlesinger.** 1998. Characterization of mannose receptor-dependent phagocytosis mediated by Mycobacterium tuberculosis lipoarabinomannan. Infect. Immun. **66:**2769–2777.
12. **Kang, P. B., A. K. Azad, J. B. Torrelles, T. M. Kaufman, A. Beharka, E. Tibesar, L. E. DesJardin, and L. S. Schlesinger.** 2005. The human macrophage mannose receptor directs Mycobacterium tuberculosis lipoarabinomannan-mediated phagosome biogenesis. J. Exp. Med. **202:**987–999.
13. **Kano, H., T. Doi, Y. Fujita, H. Takimoto, I. Yano, and Y. Kumazawa.** 2005. Serotype-specific modulation of human monocyte functions by glycopeptidolipid (GPL) isolated from Mycobacterium avium complex. Biol. Pharm. Bull. **28:**335–339.
14. **Kelley, V. A., and J. S. Schorey.** 2003. Mycobacterium's arrest of phagosome maturation in macrophages requires Rab5 activity and accessibility to iron. Mol. Biol. Cell **14:**3366–3377.
15. **Khoo, K. H., J. B. Tang, and D. Chatterjee.** 2001. Variation in mannose-capped terminal arabinan motifs of lipoarabinomannans from clinical isolates of Mycobacterium tuberculosis and Mycobacterium avium complex. J. Biol. Chem. **276:**3863–3871.
16. **Krzywinska, E., S. Bhatnagar, L. Sweet, D. Chatterjee, and J. S. Schorey.** 2005. Mycobacterium avium 104 deleted of the methyltransferase D gene by allelic replacement lacks serotype-specific glycopeptidolipids and shows attenuated virulence in mice. Mol. Microbiol. **56:**1262–1273.
17. **Kusunoki, T., E. Hailman, T. S. Juan, H. S. Lichenstein, and S. D. Wright.** 1995. Molecules from Staphylococcus aureus that bind CD14 and stimulate innate immune responses. J. Exp. Med. **182:**1673–1682.
18. **Pourshafie, M., Q. Ayub, and W. W. Barrow.** 1993. Comparative effects of Mycobacterium avium glycopeptidolipid and lipopeptide fragment on the function and ultrastructure of mononuclear cells. Clin. Exp. Immunol. **93:** 72–79.
19. **Powlesland, A. S., E. M. Ward, S. K. Sadhu, Y. Guo, M. E. Taylor, and K. Drickamer.** 2006. Widely divergent biochemical properties of the complete set of mouse DC-SIGN-related proteins. J. Biol. Chem. **281:**20440–20449.
20. **Shimada, K., H. Takimoto, I. Yano, and Y. Kumazawa.** 2006. Involvement of mannose receptor in glycopeptidolipid-mediated inhibition of phagosome-lysosome fusion. Microbiol. Immunol. **50:**243–251.
21. **Stahl, P. D., and R. A. Ezekowitz.** 1998. The mannose receptor is a pattern recognition receptor involved in host defense. Curr. Opin. Immunol. **10:**50–55.
22. **Sturgill-Koszycki, S., U. E. Schaible, and D. G. Russell.** 1996. Mycobacterium-containing phagosomes are accessible to early endosomes and reflect a transitional state in normal phagosome biogenesis. EMBO J. **15:**6960–6968.
23. **Sweet, L., and J. S. Schorey.** 2006. Glycopeptidolipids from Mycobacterium avium promote macrophage activation in a TLR2- and MyD88-dependent manner. J. Leukoc. Biol. **80:**415–423.
24. **Sweet, L., W. Zhang, H. Torres-Fewell, A. Serianni, W. Boggess, and J. Schorey.** 2008. Mycobacterium avium glycopeptidolipids require specific acetylation and methylation patterns for signaling through toll-like receptor 2. J. Biol. Chem. **283:**33221–33231.
25. **Torrelles, J. B., A. K. Azad, and L. S. Schlesinger.** 2006. Fine discrimination in the recognition of individual species of phosphatidyl-myo-inositol mannosides from Mycobacterium tuberculosis by C-type lectin pattern recognition receptors. J. Immunol. **177:**1805–1816.
26. **Vergne, I., J. Chua, H. H. Lee, M. Lucas, J. Belisle, and V. Deretic.** 2005. Mechanism of phagolysosome biogenesis block by viable Mycobacterium tuberculosis. Proc. Natl. Acad. Sci. U. S. A. **102:**4033–4038.
27. **Vergne, I., J. Chua, S. B. Singh, and V. Deretic.** 2004. Cell biology of mycobacterium tuberculosis phagosome. Annu. Rev. Cell Dev. Biol. **20:**367–394.
28. **Via, L. E., D. Deretic, R. J. Ulmer, N. S. Hibler, L. A. Huber, and V. Deretic.** 1997. Arrest of mycobacterial phagosome maturation is caused by a block in vesicle fusion between stages controlled by rab5 and rab7. J. Biol. Chem. **272:**13326–13331.

Editor: J. L. Flynn